Pertanika J. Sci. & Technol. 29 (2): 885 - 893 (2021)

SCIENCE & TECHNOLOGY

Journal homepage: http://www.pertanika.upm.edu.my/

Photonics Rib Waveguide Dimension Dependent Charge Distribution and Loss Characterization

Angie Teo Chen Chen, Mohammad Rakib Uddin* and Foo Kui Law

Electrical and Electronic Engineering Programme Area, Faculty of Engineering, Universiti Teknologi Brunei, BE1410 Brunei Darussalam

ABSTRACT

The simulation of behaviour of the charge distribution and the loss characteristic for rib-waveguide is demonstrated by using silicon-on-insulator (SOI). In this simulation, the rib waveguide is designed at a core width of 450nm, core height of 250nm, rib height of 50nm and buried oxide height of 100nm. These dimensions are set as reference. The aspiration of designing rib waveguide instead of other type of waveguide such as ridge waveguide is from the higher light confinement that can be accomplished by rib waveguide as the refractive index difference is huge and the designing of an active device can be realized. In this analysis, free carrier-injection effect was implemented in the first part of the simulation to study the distribution charges of rib-based waveguide structure based on basic dimensions. In this analysis, electrical voltage was varied from 0V to 1.2V in steps of 0.2V for the analysis of distribution of electron. In the second part of the simulation, four design parameters had been amended which included the core width and height, rib height and buried oxide height. Physical dimensions of the waveguide were altered to achieve smaller device footprint with optimized performance affecting large Free Spectral Range (FSR) and high Q-factor. With proper waveguide physical dimensions design, a good performance Micro-Ring Resonator (MRR) exhibits the principles of wide FSR and Q-factor can be achieved.

Keywords: Carrier injection; distribution of free charges; physical dimensions; rib-based waveguide structure

ARTICLE INFO

Article history:
Received: 28 September 2020
Accepted: 06 January 2021
Published: 30 April 2021

DOI: https://doi.org/10.47836/pjst.29.2.10

E-mail addresses:
angie_teo236@hotmail.com (Angie Teo Chen Chen)
rakib.uddin@utb.edu.bn (Mohammad Rakib Uddin)
p20171002@student.utb.edu.bn (Foo Kui Law)
* Corresponding author

INTRODUCTION

In the past ten years, silicon photonics have become well known as an encouraging technology for the integration of optical

ISSN: 0128-7680
e-ISSN: 2231-8526

functionalities within microelectronic chips in which various distinct components have already been presented (Lim et al., 2013; VenNatesh et a., 2016). These includes optical filters, modulators, receivers, and converter of wavelengths (Marchetti et al., 2017; Thomson et al., 2016). Nowadays, an optical MRR has become one of the constitutional building blocks in the development of Si photonic circuit integration such as optical filters based on tunability. Optical filter is one of the outstanding devices that is used in Wavelength-Division-Multiplexed (WDM) systems. The function of an optical filter is to select the desired wavelengths which pass only the wanted channel and leave other channels uninterrupted. In WDM systems, a high information capacity is achieved by a large bandwidth and with the use of optical filter based on MRRs, this can be further improved (Aziz et al., 2016). In addition to that , low power consumption and small device size can be achieved by MRR based optical filter.The main two important principal elements that persuade the advancement of silicon photonics are (i) the feasibility in realization of structure with enormous refractive index difference; and (ii) the exploitation of technology on silicon processing that have been readily developed and validated for microelectronic device industry which have the capability of delivering low cost silicon photonic components, at very large volumes. Silicon has a refractive index of as high as 3.5 (Haroon et al., 2012). A rib-based waveguide structure is built on silicon layer which is deposited on top of a silica layer (Bogaerts et al., 2014; Lin et al., 2007). In addition, silicon oxide can be structured with high thermal conductivity silicon. It is known both silicon refractive index and the number of free carrier charges are directly proportional to each other. With high refractive index, free carriers are also increased. With high refractive index, light modulation can take place at a faster speed with low consumption of power in silicon waveguide (Liu et al., 2007). Modulation scheme of waveguide can be categorized into three types; carrier injection, depletion and accumulation based electro-optic modulator on silicon-on-insulator (Debnath et al., 2018; Lim et al., 2015; Mulyanti et al., 2014; Qin et al., 2016). In here, carrier injection is chosen to carry out the simulation of charge distribution and the loss characteristics of rib waveguide. Previously in other reports, rib waveguide dimension studies had performed analysis on each dimension separately (such as varying only core width or core height). However, this study includes the analysis of all the dimensions (core width, core height, rib height and buried oxide height) under a single study to determine the loss relationship.

In this paper, the simulation and analysis of charge distribution and loss characteristics for SOI based rib waveguide based on free carrier-injection effect. The analysis covers the study of the distribution charges of rib-based waveguide structure based on basic dimensions. The rib waveguide analysis is chosen due to higher light confinement as the refractive index difference is high and an active device can be realized. With this basic design, further design dimension variations investigation on waveguide performance are accomplished such as varying the width and height of core, height of rib and height of buried oxide.

Rib Waveguide

Rib waveguide is designed with a similar structure as strip or ridge waveguide, yet the strip and the planer layer beneath the strip will share the same high index and is part of the core waveguide. This type of waveguide is known as rectangular waveguides in which the x direction is determined by thickness d and the y direction is determined by width w, however their shapes are not exactly rectangular.

The design of the rib waveguide is shown in Figure 1 which consists layers of silicon and silicon oxide. As seen from Figure 1, there are W, H, H_r and H_o, respectively.

Where, W is the core waveguide width,
H is the core waveguide height,
H_r is the rib waveguide height and
H_o is the buried oxide height

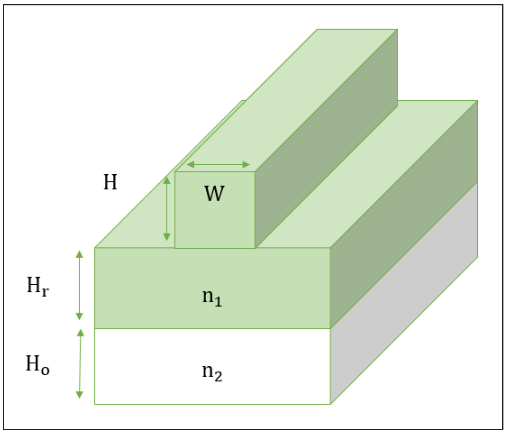

Figure 1. Rib Waveguide

METHODS

Design and Simulation of Rib Waveguide Structure

The rib-based waveguide structure on SOI platform shown in Figure 2 are designed as follows and is set as a basic reference in the entire simulation.

1. Width at 450nm – core waveguide
2. Height at 250nm – core waveguide
3. Height at 50nm – rib waveguide
4. Height at 1000nm – buried oxide

In here, rib waveguide carrier charge distribution is investigated by using a software named Lumerical DEVICE whereas the loss with respect to various dimensions is accomplished by using MODE software.

Figure 3 demonstrates the cross section of the rib waveguide where the connection of voltage source is shown. The addition of an electrical voltage source is to enhance electro-optic to occur in the waveguide as there are electric fields. In this design, for free carriers to diffuse within the core waveguide, there must be different in concentration of doping. Thus, the charge concentration is higher at highly doped p and n region as compared to

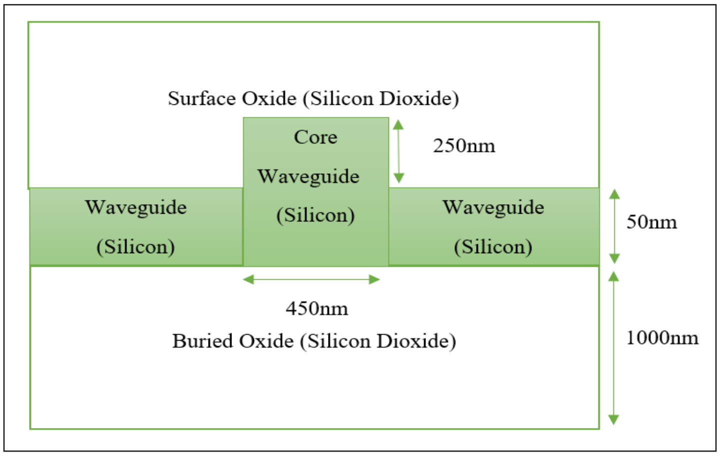

Figure 2. Waveguide block structure

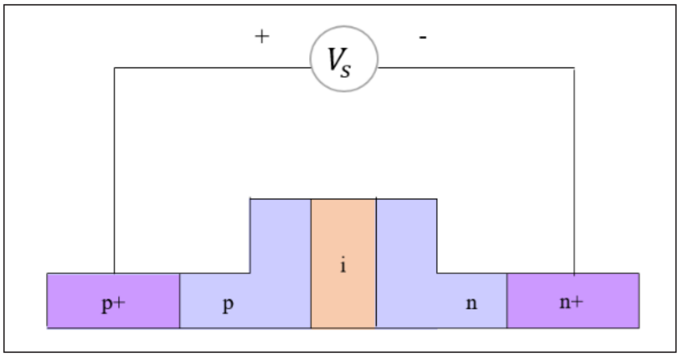

Figure 3. Cross sectional of Rib-based waveguide

the lightly doped p and n regions. Diffusion of free carriers leads to the core waveguide effective index changes.

RESULTS AND DISCUSSION

Analysis of Rib Waveguide Structure

In the first part of the simulation, the analysis of distribution of electron was carried out by varying voltage. The voltage was altered from 0 V to 1.2 V in the steps of 0.2. From the result based on Figure 4, it was observed that when there was no voltage applied, there would be no free carrier diffusion. It was seen that n free charges (red colour) slowly diffused into the p doped region (blue colour) as voltage increases. The reason of diffusion of n free charges is mainly due to the positive voltage applied to p doped region. As a result, n free charges diffused into p doped region.

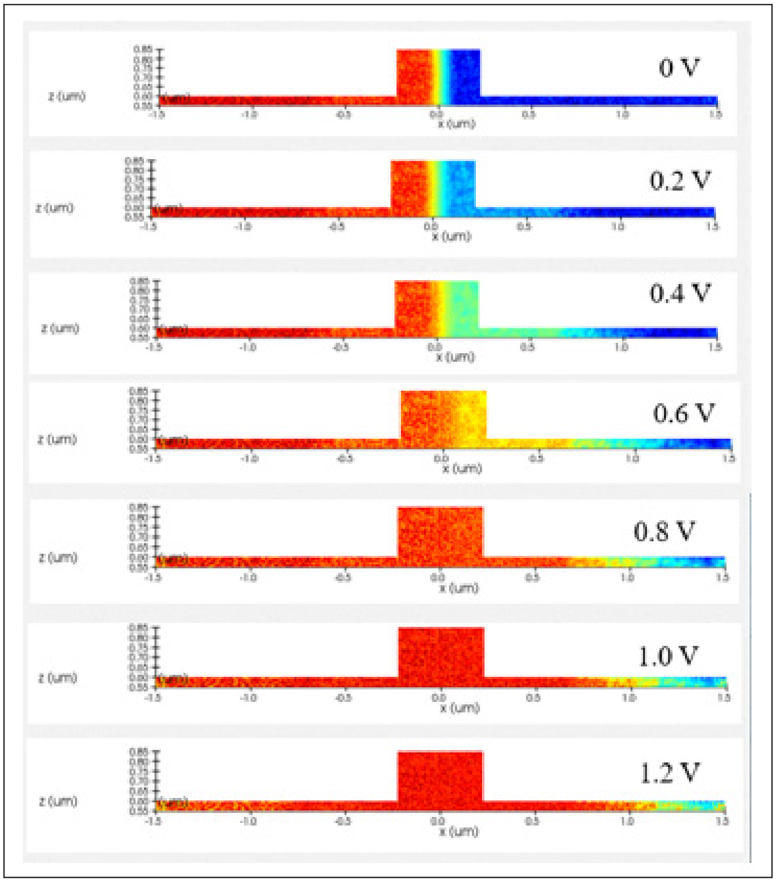

Figure 4. Distribution of charge inside the waveguide at various voltage

Simulation and Analysis Rib Waveguide Dimension Change

In the second section of the simulation, the rib-based waveguide dimensions would be varied one by one to study the performance of dimension change which included core waveguide width and height, rib waveguide height and rib waveguide height. From this, the loss characteristic graph with respect to various dimensions were obtained and analyzed.

Core Waveguide Width Change

In this part, the width of core was altered from 500nm to 700nm at the steps of 100nm in which the height of the core, rib and buried oxide were constant at 250nm, 50nm and 1000nm, respectively. Based on the results shown in Figure 5, as the core width increased, loss would also be increased. Thus, to achieve smaller loss, it is recommended to choose the core width of less than 700nm.

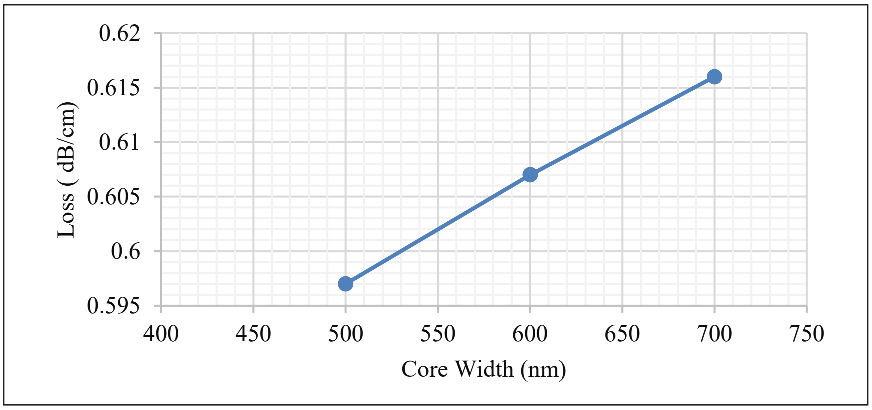

Figure 5. Loss characteristics with respect to different core width

Core Waveguide Height Change

The height of core was altered from 190nm to 230nm at the steps of 20nm in which the other dimensions remain at the basic reference value. It was noticeable that losses were directly proportional to the height of the core waveguide as shown in Figure 6. Thus, it can be determined that as we increased the height of the core waveguide, losses also increased. For this reason, it is advisable to choose a smaller core height for lower loss.

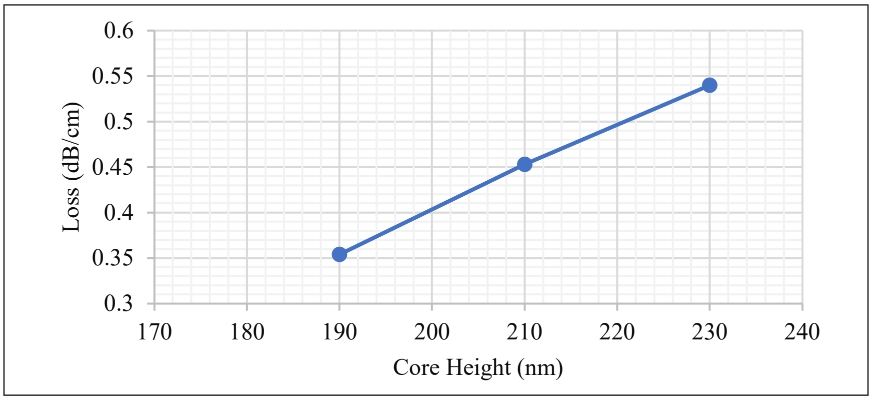

Figure 6. Loss characteristics with respect to different core height

Rib Waveguide Height Change

In this part, the height of the rib waveguide would be varied from 50nm to 90nm at the interval of 20nm in which the height of the core, rib and buried oxide were constant at 250nm, 50nm and 1000nm, respectively. The simulated results of losses with respect to rib height is shown in Figure 7. From the simulated results, it was shown that increasing the rib height would results in lower losses.

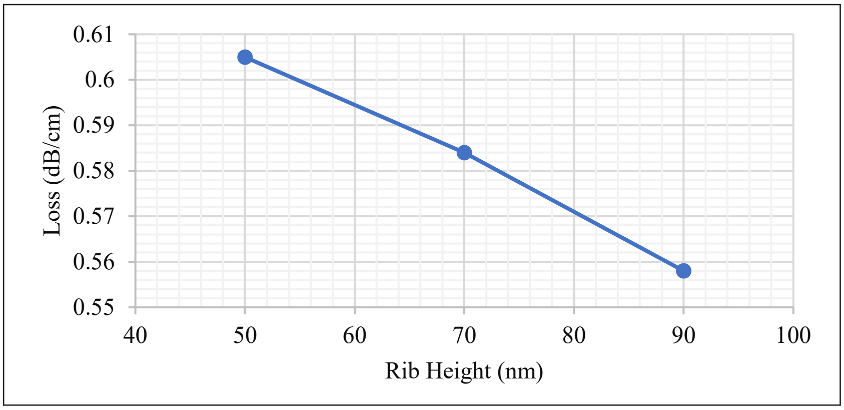

Figure 7. Loss characteristics with respect to different rib height

Buried Oxide Height Change

In this part, the height of buried oxide would be varied from 500nm to 1500nm at the interval of 500nm with all other parameters remaining constant at reference. Based on the simulated results shown in Figure 8, it was observed that there were no changes in loss as the height of buried oxide was increased from 500nm to 1500nm at an interval of 500nm.

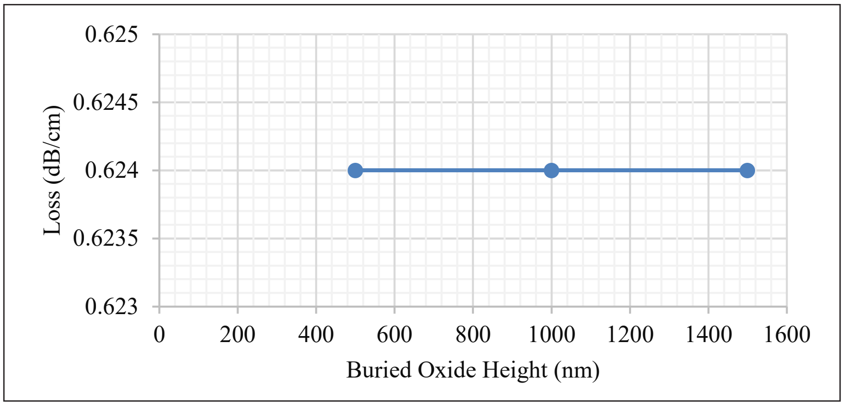

Figure 8. Loss characteristics with respect to different buried oxide height

CONCLUSION

The simulation of behaviour of the distribution of charge and the loss characteristics of rib waveguide is demonstrated by using silicon-on-insulator platform. Free carrier-injection effect is used in the simulation of distribution of charge by the means of varying electrical voltage. In here, the range of voltage changes in the steps of 0.2 V from 0V to 1.2V for examining distribution of electron. Once charge distribution is achieved by Lumerical DEVICE solution, parameters such as loss is further obtained by Lumerical MODE solution.

From there on, further design dimension variations investigation on waveguide performance are accomplished such as varying the width and height of core, height of rib and height of buried oxide. Simulation of rib waveguide dimension change have been accomplished, and graphs haven been plotted to present the results. From the graphs plotted, we can clearly see how each dimension can affect the loss characteristic. It is seen that as core width and core height increases, more losses will be achieved. On the other hand, smaller rib height will lead to lower losses. Simulations have also shown that height of buried oxide does not have significant effect on loss of the waveguide, this means that there is no change in loss as we vary the height of buried oxide. As we know the performance of the waveguide not only depends on loss but there are also other factors. Therefore, in terms of loss, it is deduced that smaller rib height, larger width core and larger height core will lead to more losses. As a conclusion, with this analysis we can determine the variables to maximize the efficiency of rib wave guide. This study can be used as a reference for future research designers to make fundamental decisions relating to the results obtained from these simulations so they can be more effective in designing reliable photonic devices.

ACKNOWLEDGEMENT

We would like to thank Universiti Teknologi Brunei (UTB) for financial support to carry on this research.

REFERENCES

Aziz, N. N. A., & Haroon, H., & Razak, H. A. (2016). Compact optical filter based on microring resonator. *ARPN Journal of Engineering and Applied Sciences, 11*(5), 3320-3323.

Bogaerts, W., Fiers, M., & Dumon, P. (2014). Design challenges in silicon photonics. *IEEE Journal of Selected Topics in Quantum Electronics, 20*(4), Article 8202008. https://doi.org/ 10.1109/JSTQE.2013.2295882.

Debnath, K., Thomson, D. J., Zhang, W., Khokhar, A. Z., Littlejohns, C., Byers, J., Mastronardi, L., Husain, M. K., Ibukuro, K., Gardes, F. Y., Reed, G. T., & Saito, S. (2018). All-silicon carrier accumulation modulator based on a lateral metal-oxide-semiconductor capacitor. *Photonics Research, 6*(5), 373-379. https://doi.org/10.1364/PRJ.6.000373

Haroon, H., Shaari, S., Menon, P., Mardiana, B., Hanim, A., Arsad, N., Majlis, B., Mukhtar, W., & Abdullah, H. (2012). Design and characterization of multiple coupled microring based wavelength demultiplexer in silicon–on–insulator (SOI). *Journal of Nonlinear Optical Physics & Materials*, 21(1), Article 1250004. https://doi.org/10.1142/S021886351250004X

Lim, A. E. J., Song, J., Fang, Q., Li, C., Tu, X., Duan, N., Chen, K. K., Tern, R. P. C., & Liow, T. Y. (2013). Review of silicon photonics foundry efforts. *IEEE Journal of Selected Topics in Quantum Electronics, 20*(4), 405-416. https://doi.org/10.1109/JSTQE.2013.2293274

Lim, S. T., Sun, M. J., & Png, C. E. (2015). Silicon optical modulator simulation. *Frontiers in Physics, 3*, Article 27. https://doi.org/10.3389/fphy.2015.00027

Lin, Q., Painter, O. J., & Agrawal, G. P. (2007). Nonlinear optical phenomena in silicon waveguides: Modeling and applications. *Optics express, 15*(25), 16604-16644. https://doi.org/10.1364/OE.15.016604

Liu, A., Liao, L., Rubin, D., Nguyen, H., Ciftcioglu, B., Chetrit, Y., Izhaky, N., & Paniccia, M. (2007). High-speed optical modulation based on carrier depletion in a silicon waveguide. *Optics express, 15*(2), 660-668. https://doi.org/10.1364/OE.15.000660

Marchetti, R., Vitali, V., Lacava, C., Cristiani, I., Giuliani, G., Muffato, V., Fournier, M., Abrate, S., Gaudino, R., Temporiti, E., Carroll, L., & Minzioni, P. (2017). Low-loss micro-resonator filters fabricated in silicon by CMOS-compatible lithographic techniques: design and characterization. *Applied Sciences, 7*(2), Article 174. https://doi.org/10.3390/app7020174

Mulyanti, B., Menon, P. S., Shaari, S., Hariyadi, T., Hasanah, L., & Haroon, H. (2014). Design and optimization of coupled Microring Resonators (MRRs) in silicon-on-insulator. *Sains Malaysiana, 43*(2), 247-252.

Qin, Y., Yu, Y., Wu, W., & Zhang, X. (2016). Integrated tunable optical add/drop filter for polarization and wavelength multiplexed signals. *Optics Express, 24*(7), 7069-7078. https://doi.org/10.1364/OE.24.007069

Thomson, D., Zilkie, A., Bowers, J. E., Komljenovic, T., Reed, G. T., Vivien, L., & Nedeljkovic, M. (2016). Roadmap on silicon photonics. *Journal of Optics, 18*(7), Article 073003. https://doi.org/10.1088/2040-8978/18/7/073003

VenNatesh, B. S., Britto, E. R. A., & Balaji, S. S. (2016). *Overview of Silicon Photonic Signal Processing*. Citeseer Sastra University. Retrieved October 4, 2020, from http://citeseerx.ist.psu.edu/viewdoc/download?doi=10.1.1.857.5778&rep=rep1&type=pdf